**Original Article** | Gastrointestinal Imaging

http://dx.doi.org/10.3348/kjr.2014.15.2.235
pISSN 1229-6929 · eISSN 2005-8330
Korean J Radiol 2014;15(2):235-244

Korean Journal of Radiology
KJR

# Monopolar Radiofrequency Ablation Using a Dual-Switching System and a Separable Clustered Electrode: Evaluation of the *In Vivo* Efficiency

Jeong Hee Yoon, MD[1], Jeong Min Lee, MD, PhD[1, 2], Eui Jin Hwang, MD[1], In Pyung Hwang, MD[1], Jeehyun Baek, MD[1], Joon Koo Han, MD[1, 2], Byung Ihn Choi, MD[1, 2]

[1]Department of Radiology, Seoul National University Hospital, Seoul 110-744, Korea; [2]Institute of Radiation Medicine, Seoul National University College of Medicine, Seoul 110-744, Korea

**Objective:** To determine the *in vivo* efficiency of monopolar radiofrequency ablation (RFA) using a dual-switching (DS) system and a separable clustered (SC) electrode to create coagulation in swine liver.

**Materials and Methods:** Thirty-three ablation zones were created in nine pigs using a DS system and an SC electrode in the switching monopolar mode. The pigs were divided into two groups for two experiments: 1) preliminary experiments (n = 3) to identify the optimal inter-electrode distances (IEDs) for dual-switching monopolar (DSM)-RFA, and 2) main experiments (n = 6) to compare the *in vivo* efficiency of DSM-RFA with that of a single-switching monopolar (SSM)-RFA. RF energy was alternatively applied to one of the three electrodes (SSM-RFA) or concurrently applied to a pair of electrodes (DSM-RFA) for 12 minutes in *in vivo* porcine livers. The delivered RFA energy and the shapes and dimensions of the coagulation areas were compared between the two groups.

**Results:** No pig died during RFA. The ideal IEDs for creating round or oval coagulation area using the DSM-RFA were 2.0 and 2.5 cm. DSM-RFA allowed more efficient RF energy delivery than SSM-RFA at the given time (23.0 ± 4.0 kcal vs. 16.92 ± 2.0 kcal, respectively; $p = 0.0005$). DSM-RFA created a significantly larger coagulation volume than SSM-RFA (40.4 ± 16.4 $cm^3$ vs. 20.8 ± 10.7 $cm^3$; $p < 0.001$). Both groups showed similar circularity of the ablation zones ($p = 0.29$).

**Conclusion:** Dual-switching monopolar-radiofrequency ablation using an SC electrode is feasible and can create larger ablation zones than SSM-RFA as it allows more RF energy delivery at a given time.

**Index terms:** *Liver; Interventional procedures; Thermal ablation; Radiofrequency ablation; Experimental study*

## INTRODUCTION

Radiofrequency ablation (RFA) has gained wide acceptance as a minimally invasive therapeutic alternative to surgical treatment for hepatocellular carcinomas (HCCs) < 5 cm in diameter (1-3). According to the updated Barcelona Clinic Liver Cancer staging system, RFA is the most preferred treatment for very early stage HCC of < 2 cm in diameter or early stage HCC ≤ 3 cm in patients with portal hypertension or with significant co-morbidity (4). Monopolar RFA using a single electrode is currently the most commonly used thermal ablation technique (3), and complete ablation by percutaneous RFA shows a good long-term outcome in > 90% of treated patients for lesions < 2 cm (5-7). However, one of the major limitations of RFA is its higher rate of local tumor progression than that seen after surgical resection due to its inability to reliably create an adequate ablation volume (6, 8-13). Although a systematic review (14)

Received June 30, 2013; accepted after revision January 11, 2014.
This study is partly supported by STARmed Co., Ltd.
**Corresponding author:** Jeong Min Lee, MD, PhD, Department of Diagnostic Radiology, Seoul National University Hospital, 101 Daehak-ro, Jongno-gu, Seoul 110-744, Korea.
• Tel: (822) 2072-3154 • Fax: (822) 743-6385
• E-mail: jmsh@snu.ac.kr

demonstrated better local control in HCCs > 2 cm treated by RFA compared with that of an ethanol injection, a long-term effectiveness study demonstrated that RFA showed significantly higher local tumor progression (20.5%) than that of surgical resection (0.4%) (15).

Despite the recent development of several new monopolar RFA devices with greater efficiency for creating large ablation zones, treatment of liver tumors > 3 cm in diameter often requires multiple, overlapping ablations to create sufficient ablation margins around index tumors (16-18). However, it is technically challenging to place an electrode in the remaining tumor portion during overlapping ablations under ultrasound guidance due to gas bubble formation (19, 20). To overcome this technical difficulty of overlapping ablation and to generate larger ablation zones than RFA using a single electrode, multiple-electrode RF systems such as the switching controller (Valleylab, Boulder, CO, USA), the multi-channel RF generator (STARmed Co., Ltd., Goyang, Korea), and the multipolar RF system (Celon, Teltow, Germany) have been introduced and are commercially available (21-23). Several previous studies of monopolar RFA using a multiple-electrode switching system have shown its efficiency for creating a larger ablation zone in the liver than could be created using the standard monopolar RF technique (20, 24, 25). Yoon et al. (26) demonstrated that a combination of dual-switching monopolar (DSM)-RFA using a separable clustered (SC) electrode (Octopus®; STARmed Co., Ltd., Goyang, Korea) and a prototype, three-channel, dual-generator RFA unit having an impedance-controlled automatic switching mechanism, create a significantly larger ablation volume than does the consecutive mode in *ex vivo* bovine liver (27). However, there has been no *in vivo* study until now that has demonstrated the *in vivo* efficiency of using a prototype, three-channel, dual-generator RFA unit that allows simultaneous delivery of maximum RF energy of 200 W to two electrodes. Therefore, the purpose of this study was to determine the optimal inter-electrode distances (IEDs) for creating a large, unified ablation zone in the liver by DSM-RFA and to compare the *in vivo* efficiency of DSM-RFA with that of single-switching monopolar (SSM)-RFA.

## MATERIALS AND METHODS

Financial support and the investigational RFA device for this study were provided by STARmed Co., Ltd. The authors had complete control of the data and information submitted for publication, which was unbiased by industry.

### RFA System and Electrode

A three-channel DSM generator (VIVA Multi®; STARmed Co., Ltd., Goyang, Korea) (Fig. 1A) and an SC electrode (Octopus®; STARmed) were used to maximize the delivery of RF energy within a given time. The details of the three-channel DSM-RFA unit and the SC electrode have been described in some previous studies (25, 26). Briefly, the DSM-RFA unit features simultaneous RF energy delivery to two electrodes using two, independent, 200 W generators at a frequency of 480 kHz and is able to automatically switch the RF energy between the two pairs of three electrodes according to impedance changes similar to those of an SSM-RFA system (25, 26). The SC electrode is composed of three, cooled-tip electrodes with a 2.5-cm active tip (Fig. 1B). The SC electrode is similar to a clustered electrode, although it differs from a conventional clustered electrode in that each individual electrode is separable (28). The SC

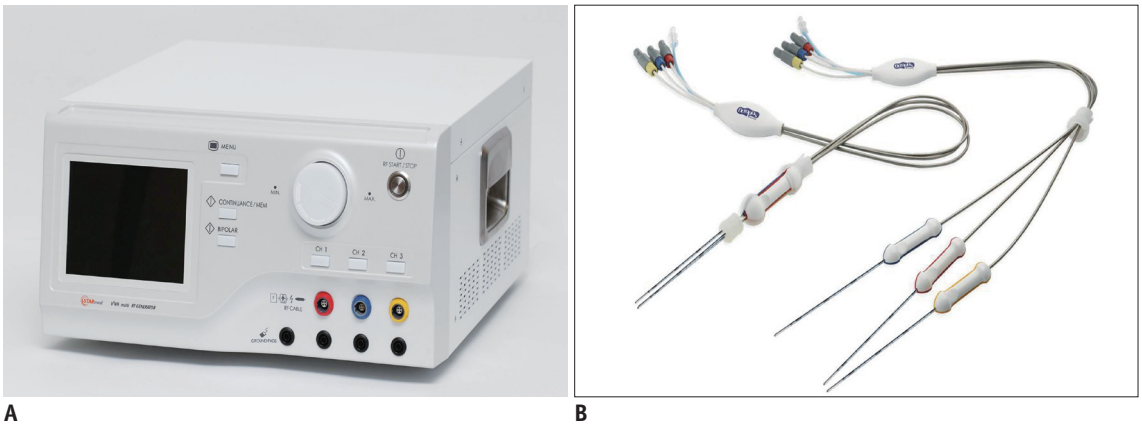

A B

**Fig. 1. Prototype three-channel, dual-generator radiofrequency ablation unit (A) and single separable clustered (Octopus®) electrode (B).**

Korean Journal of Radiology
KJR

electrode can be placed as a single electrode with variable IEDs, according to the shape and size of the target tumor. Therefore, depending on the operator's intention, the three electrodes of the SC electrode can be used as three internally cooled electrodes for SSM- or DSM-RFA when they are separated, whereas the SC electrode in a single body can be used for conventional monopolar RFA. In this study, 165 W of maximum output for each generator was delivered to two tips of an SC electrode (330 W in total) when we performed DSM-RFA.

### Anesthesia and Intraoperative RFA

This protocol was approved by the Animal Use and Care Administrative Advisory Committee of our medical institution, and all experiments were performed according to the institutional guidelines for the care and use of laboratory animals. Nine domestic male pigs (weight: 65–80 kg, mean weight, 70 kg) underwent intraoperative RFA under general anesthesia using isoflurane (IsoFlo, Abbott Laboratories, Abbott Park, IL, USA) following an intramuscular injection of 30 mg/kg of zolazepam hydrochloride (Zoletil, Virbac, Carros, France) and 5 mg/kg of xylazine (Rompun, Bayer Korea, Ansan, Korea). An upper midline incision was made from the xiphoid process to the umbilicus. Two radiologists, one attending radiologist with 15 years of RFA experience and one third-year radiology resident performed all of the ablations under intraoperative ultrasound guidance using an Accuvix V10 scanner (Samsung Medison, Seoul, Korea) with a high-frequency, linear-array, broadband L6–12 IS transducer (Samsung Medison, Seoul, Korea). The three tips of the SC electrode were placed in the liver under ultrasound guidance while avoiding the large hepatic vein and portal veins. Three to four RFA zones were made per each pig liver depending on the size of the liver.

The nine pigs were allocated into two studies: 1) preliminary experiments (n = 3) to identify IEDs for DSM-RFA, and 2) the main experiments (n = 6) to compare the *in vivo* efficiency of DSM-RFA with that of SSM-RFA.

### Preliminary Experiments to Identify the Optimal IED

Three pigs were used to identify the optimal IEDs for DSM-RFA. Using a 17-G SC electrode and the three-channel DSM-RF generator, a total of nine RF-induced ablation zones were created in three pigs, with various IEDs (2.0–3.5 cm): 2.0 cm (n = 2); 2.5 cm (n = 2); 3.0 cm (n = 3); and 3.5 cm (n = 2) (Fig. 2). RF energy was simultaneously delivered to a pair of electrodes from the two generators for 12 minutes at the maximum wattage of 165 W (330 W in total) using an impedance-controlled algorithm. During the procedure, the temperature of the electrode tip and the impedance were continuously measured by the RFA unit. The shapes of the ablation zones at the different IEDs were classified into three groups: oval/round; triangular-shaped with or without indentation (heart- or maple-leaf-shaped); or separated. In addition, the minimum, maximum, and vertical diameters of the ablation zones were measured if an ablation zone was united into an oval/round shape.

### Main Experiments

#### *Ablation Protocol for the Main Study*

Based on the preliminary results, the main study was conducted to compare the *in vivo* efficiency of DSM-RFA with that of SSM-RFA, as seen in six pigs. In each pig, we created two ablation zones using the SSM mode and DSM mode (a total of four ablation zones). In addition, to avoid any influence of the location of the ablation zone on ablation volume, we changed the location of the ablation zones across the pigs. Therefore, we created a total of six ablation lesions in the right lobe and six lesions in the left lobe for each of the SSM mode and DSM mode. The three electrode tips of the SC electrode were placed into the swine liver through the holes of a triangular acrylic plate with 2.0 cm or 2.5 cm of equidistant inter-electrode spacing. The RF energy (maximum 200 W) was applied to one of the three electrodes for those RFA zones created with the SSM technique and was switched into the three electrode tips of the SC electrode for a total of 12 minutes in the impedance control mode, as described in a previous study (Fig. 3A) (26). The DSM technique to create the other group of RFA zones was actually a combined use of the DSM mode and SSM mode. RF energy (maximum 330 W in total; 165 + 165 W each) was initially applied simultaneously to the three possible pairs of electrodes of the SC electrode in a switching pattern until the impedance rose > 170% of the initial impedance (initial roll off). Then, maximum RF energy up to 200 W for each electrode was allowed, although RF energy was alternatively delivered in DSM and SSM modes (Fig. 3B). The reason we restricted the maximum RF energy delivery up to a maximum of 330 W until the impedance rise was to avoid a potential early impedance rise caused by char formation around the electrodes. Similarly, we alternated the DSM and SSM modes to prevent too rapid impedance rises during the RFA session, as caused

by too much of a high electrical current deposit around the electrodes, and also to avoid impedance rises due to possible electrical interference in DSM mode. Therefore, RF energy was delivered to the target tissue in DSM mode for 70–75% of the procedure time and in SSM mode for the remaining time. Switching of RF energy delivery between

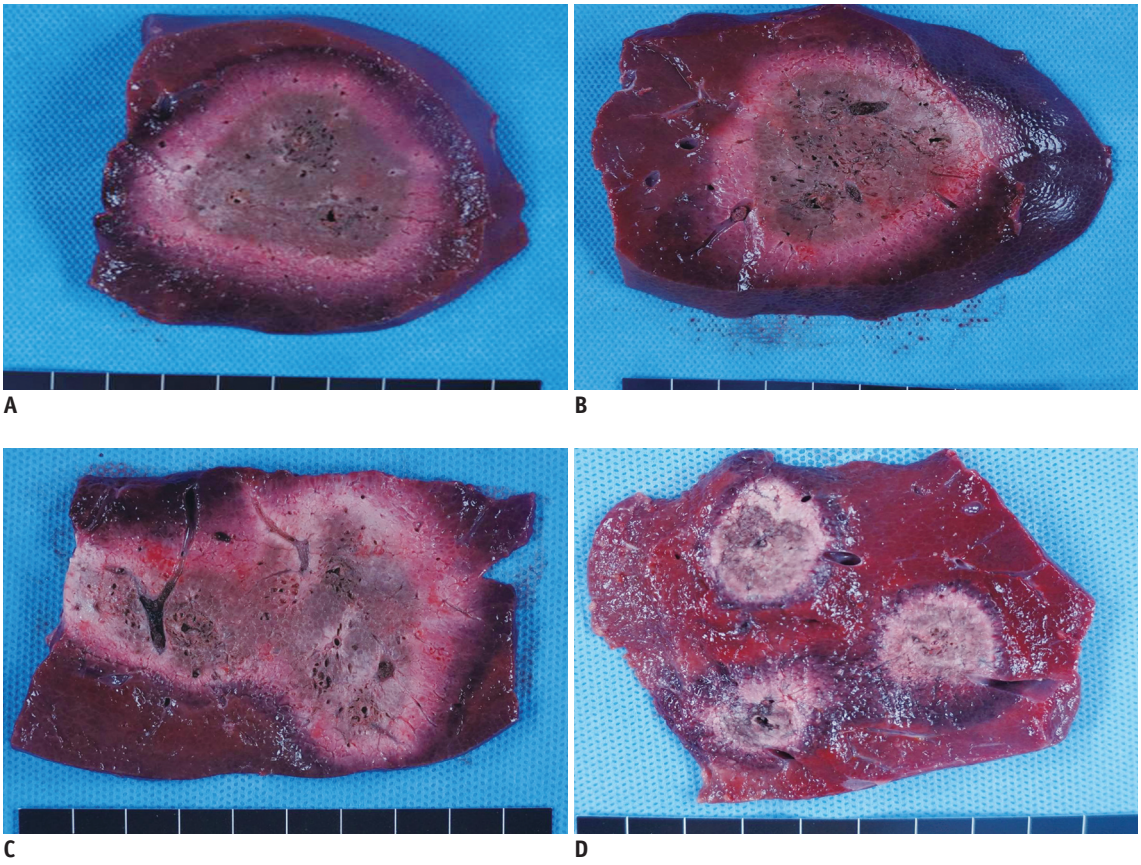


**Fig. 2. Comparison of ablation zones created by dual-switching monopolar radiofrequency ablation (DSM-RFA) at inter-electrode distances (IEDs) of 2.0 cm (A), 2.5 cm (B), 3.0 cm (C), and 3.5 cm (D).**
Note that ablation zones created in DSM-RFA at 2.0 cm and 2.5 cm IEDs showed united, round/oval-shaped lesions **(A, B)**, although ablation zones at 3.0 cm and 3.5 cm IEDs were separated **(C, D)**.

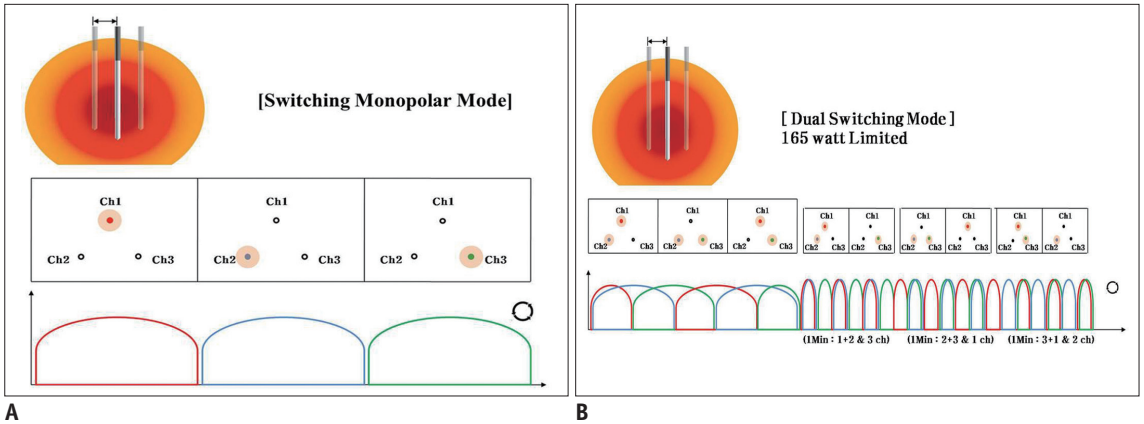


**Fig. 3. Diagrams of radiofrequency (RF) energy delivery patterns during single-switching monopolar (SSM)-radiofrequency ablation (RFA) (A) and dual-switching monopolar (DSM)-RFA (B).**
**A.** SSM-RFA: RF energy (maximum 200 W) was applied to one of three electrodes and was switched among three electrode tips of SC electrode, depending on tissue impedance changes, for total of 12 minutes. **B.** DSM-RFA: synchronous parallel RF energy (maximum 330 W; 165 + 165 W) was applied to pair of three electrodes, and RF energy was delivered in alternating fashion to possible three pairs of electrodes of SC electrode, similar to SSM-RFA.

Korean Journal of Radiology
KJR

the pair of electrodes was automatically controlled by the RFA unit by continuous monitoring of the impedance values of all of the electrodes. Consequently, continuous RF energy delivery was achieved during the RFA procedure in both modes (29).

### Lesion Size Measurement and Shape Analysis

All pigs were sacrificed by intravenous injection of potassium chloride following the RFA procedures, and all livers were removed en bloc. Each liver lobe containing RFA-induced coagulation was divided and sliced in the axial plane perpendicular to the electrode tracks. A histopathologic study for coagulation specimens was performed, including staining for mitochondrial enzyme activity by incubating the representative tissue sections for 30 minutes in 2% 2,3,5-triphenyl tetrazolium chloride (Sigma, St. Louis, MO, USA) at 20°C to 25°C as described in our previous study (28). This test was performed to determine the possibility of irreversible cellular injury sustained during the early stages of RF-induced necrosis (30). After staining, the slices were placed on an optical platform and photographs were obtained with a commercial digital camera (Canon EOS 30D; Canon Inc., Tokyo, Japan). Analysis of the diameters and shapes of the ablation zones was performed using Image J software as described in a previous study (http://rsbweb.nih.gov/ij) (26).

One observer with 2 years experience performing *in vivo* experimental RFA studies who was blinded to the information regarding the RFA techniques used in the study, measured the maximum ($D_M$) and minimum ($D_m$) diameters of the central white region of the RFA zones on the slice showing the maximum coagulation area. In addition, the liver block was also sliced along the electrode track, and the vertical diameter ($D_v$) of the central white region of the RFA zones was measured. The volumes of the RF zones as well as the effectively ablated volumes ($Volume_{eff}$) were determined using the following formulas (8):

$Volume = \pi / 6 \times D_M \times D_m \times D_v$; and

$Volume_{eff} = 4 / 3 \times \pi \times (D_m / 2)^3$.

A representative slice of the ablation zones were fixed in 10% formalin for routine histological processing, and hematoxylin-eosin staining was performed for histological assessment.

### Statistical Analysis

The normal distribution of the three diameters, $D_M$, $D_m$, and $D_v$, the volumes of the ablation zones, and the technical parameters of the SSM and DSM groups were tested using the Kolmogorov-Smirnov test. The dimensions of the ablation zones and the RF energy delivered to the two groups were compared using the paired *t* test. The shape of ablation zones was compared between the two groups. A $p$ value < 0.05 was considered significant. The statistical analysis was performed using MedCalc ver. 12 (MedCalc Software, Acacialaan, Belgium).

## RESULTS

### Intraoperative Findings and Gross and Histopathologic Results

All nine pigs tolerated the RFA procedures in the SSM or DSM mode under laparotomy. No pig showed major procedural-related changes in their vital signs on an electrocardiogram when a maximum 330 W of RF energy was delivered to a pair of active tips of an SC electrode. No significant post-RFA complications were observed such as bleeding or damage to other internal organs. In all cases, the operators were able to see the color changes of the liver capsule overlying the ablated zones within 3 minutes after starting the RFA procedure. Intraoperative ultrasound also showed typical echogenic clouds in the RFA-created ablation zones. Three cases showed thrombosis of peripheral hepatic vein branches (two DSM-RFA cases and one SSM-RFA case at 2.5 cm of IED) on intraoperative ultrasound and later confirmed by necropsy. However, no case of major portal venous thrombosis was seen on intra-operative ultrasonography or at necropsy.

Overall, the ablation zones created by DSM-RFA and SSM-RFA showed round or triangular shapes, and the ablation zones along each electrode tip were united. However, in seven cases (preliminary study [n = 4] and main study [n = 3]) normal-looking, intervening areas were observed between the ablation zones along the individual tips of the SC electrode, and these lesions were classified as a "separated" group.

In all cases, the RFA-induced ablation zones showed typical acute RFA-induced histopathological changes as a central necrotic zone surrounded by a peripheral hemorrhagic zone consisting of necrotic hepatocytes, interstitial hemorrhage, and polymorphonuclear leukocyte infiltrates (31).

### Preliminary Study to Determine the Ideal IEDs

Among the nine coagulation lesions that were created

by DSM-RFA with IEDs of 2.0–3.5 cm, five lesions (55.5%) were united and oval/round shaped, although four lesions (44.5%) were completely or partially separated. At 2.0-cm and 2.5-cm IEDs, the ablation zones were united (Fig. 2A, B), whereas all ablation zones were separated at 3.5-cm IED, and only one lesion was unified at 3.0-cm IED (1/3, 33.3%) (Fig. 2C, D). No difference in the ratio of $D_m/D_M$ of the ablation zones was observed between the 2.0-cm (0.93) and 2.5-cm IEDs (0.94). Therefore, 2.0-cm and 2.5-cm IEDs were regarded as an acceptable condition for DSM-RFA and were selected for the main study comparing the *in vivo* efficiency of DSM-RFA and SSM-RFA.

### SSM-RFA and DSM-RFA Technical Parameters

The mean impedance of the SSM-RFA and DSM-RFA groups, which was monitored during the RFA procedures, was in 62–67 ohm. No difference in the mean impedance value was observed between the two groups (65.1 ± 8.2 ohm in DSM-RFA vs. 63.5 ± 7.6 ohm in SSM-RFA; $p$ = 0.37). The mean value of the total delivered RF energy was significantly higher in the DSM-RFA (23.0 ± 4.0 kcal) than that in the SSM-RFA (16.9 ± 2.0 kcal) ($p < 0.0001$). Furthermore, DSM-RFA was more efficient for delivering RF energy per minute than the SSM mode; mean delivered RF energy per minute was 1.9 kcal/min for DSM-RFA and 1.4 kcal/min for SSM-RFA ($p < 0.0001$).

### Size Measurement and Shape Analysis of the Ablation Zones

Among the 12 ablation zones in DSM-RFA at 2.0-cm or 2.5-cm IED, all lesions generated unified ablation zones along the three electrodes; no lesions showed normal-looking intervening liver parenchyma. However, SSM-RFA induced three separated ablation zones (3/12, 25%) at 2.5-cm IED, and the remaining nine ablation zones (9/12, 75%) were united. Eight round/oval-shaped lesions (8/12; 75%) were observed in the DSM group and four triangular lesions with an indentation or heart shape were observed in the SSM group (4/12; 25%) (Table 1, Fig. 4A, B). Only four lesions (4/9; 44.4%) showed a united and round/oval shape in the SSM group. Five lesions (5/9; 55.6%) were united but showed a triangular shape with or without indentation (heart or maple leaf shapes) (Fig. 4C), and the remaining three were separated (Fig. 4D). Although DSM-RFA created more unified lesions with a round/oval shape than did SSM-RFA, no significant difference was observed in the unified ablation zone incidence between the two techniques ($p$ = 0.22). The ratios of $D_M/D_m$ of the united ablation zones in the DSM group and the SSM group were 0.9 ± 0.1, and 0.810 ± 0.1, respectively ($p$ = 0.29).

All ablation zones (6/6; 100%) created at 2.0-cm IED in the DSM group showed a round/oval shape, although only two ablation zones (2/6; 25%) were round/oval shaped at 2.5-cm IED (Table 1). The other four lesions in the DSM group that were created at 2.5-cm IED were triangular-shaped with/without a waist (heart or maple leaf shapes).

In addition, the diameters ($D_M$, $D_m$, $D_v$) of the DSM group were significantly larger than those of the SSM group ($p < 0.05$) (Table 2). As a result, the mean ablation volume of the DSM group was significantly larger than that of the SSM group (DSM, 40.4 ± 16.4 $cm^3$; SSM, 20.8 ± 10.7 $cm^3$; $p < 0.001$) (Table 2). Effective ablation volume in the DSM group was also significantly larger than that in the SSM group (0.9 ± 0.1 and 0.8 ± 0.1, respectively, $p < 0.001$) (Table 2). No significant differences were observed between ablation volume and effective ablation volume in each group.

## DISCUSSION

Our results demonstrated that the DSM-RFA technique using the dual generator RF system and an SC electrode is feasible and safe. DSM-RFA creates a significantly larger

**Table 1. Distribution of Ablation Zone Shapes in Dual-Switching Monopolar (DSM)-Radiofrequency Ablation (RFA) and Single-Switching Monopolar (SSM)-RFA Groups**

| | Unified | | Separated | Total |
|---|---|---|---|---|
| | Oval/Round | Triangular | | |
| 2.0-cm-IED (%) | | | | |
| DSM-RFA | 6 (100) | 0 (0) | 0 (0) | 6 |
| SSM-RFA | 4 (66.7) | 2 (33.3) | 0 (0) | 6 |
| 2.5-cm-IED (%) | | | | |
| DSM-RFA | 2 (33.3) | 4 (66.7) | 0 (0) | 6 |
| SSM-RFA | 0 (0) | 3 (50) | 3 (50) | 6 |

**Note.**— IED = inter-electrode distance

Korean Journal of Radiology
KJR

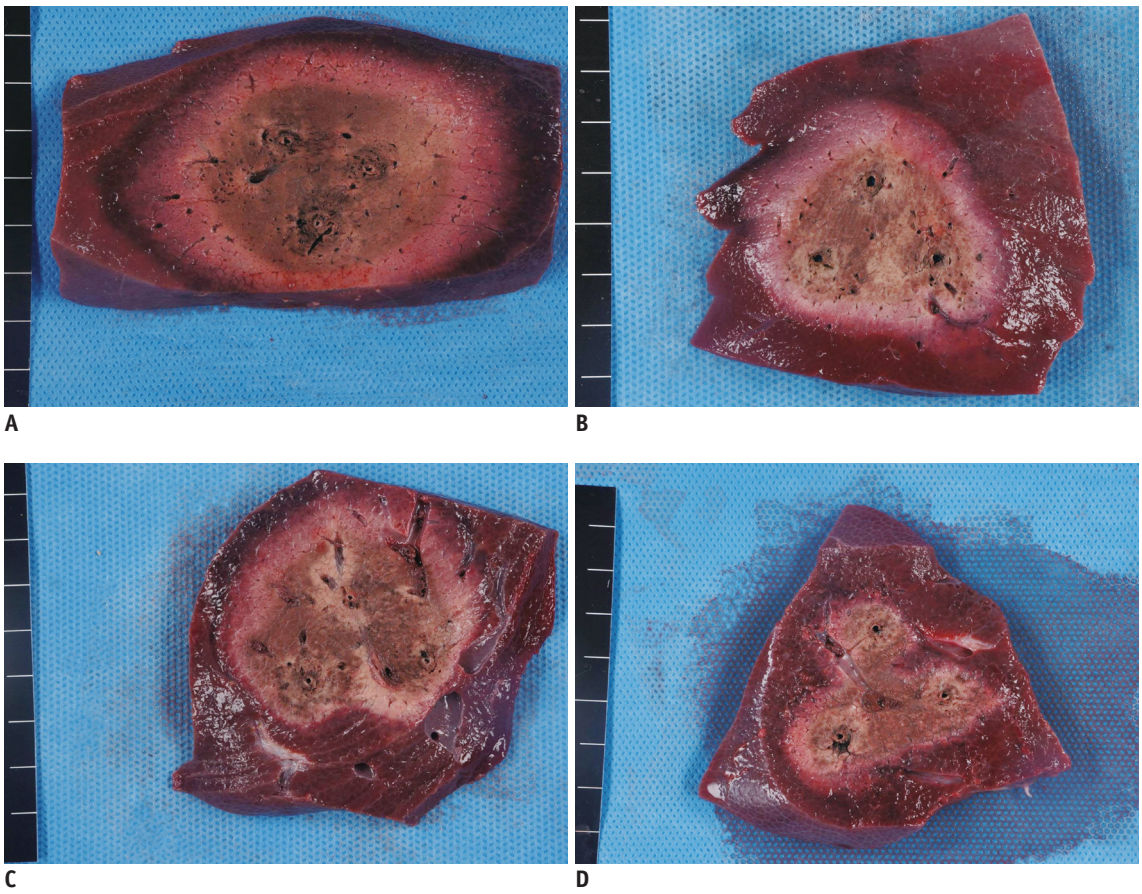


**Fig. 4. Photographs of radiofrequency ablation (RFA)-induced ablation zones created by single-switching monopolar (SSM)-RFA and dual-switching monopolar (DSM)-RFA at 2-cm or 2.5-cm inter-electrode distances (IEDs).**
**A.** Transverse cut section of specimen created in DSM-RFA with 2-cm IED. Ablation zone was approximately 6.5 x 5.0 $cm^2$. **B.** Transverse cut section of specimen created with DSM-RFA and 2.5-cm IED. Area of ablation zone was 4.5 x 5.0 $cm^2$. Note that ablation zone is triangular shaped. **C.** Transverse cut section of specimen created in SSM-RFA with 2.0-cm IED. Maximum and minimum diameters of ablation zone were 5.8 cm and 5.3 cm, respectively. **D.** Transverse cut section of specimen created in SSM-RFA with 2.5-cm IED. Note that ablation zone was separated.

**Table 2. Mean Values of Each Parameter in DSM-RFA and SSM-RFA Groups**

| Ablation Zones | DSM-RFA (n = 12) | SSM-RFA (n = 12) | *P** |
|---|---|---|---|
| $D_m$ (cm) | 4.1 ± 0.8 | 3.1 ± 0.8 | 0.006 |
| $D_M$ (cm) | 4.8 ± 0.9 | 3.9 ± 0.9 | 0.006 |
| $D_v$ (cm) | 3.8 ± 0.4 | 3.2 ± 0.5 | < 0.002 |
| Volume ($cm^3$) | 40.4 ± 16.4 | 20.8 ± 10.7 | < 0.002 |
| $Volume_{eff}$ ($cm^3$) | 40.5 ± 20.8 | 19.0 ± 11.9 | < 0.001 |
| $D_m/D_M$ ratio | 0.9 ± 0.1 | 0.8 ± 0.1 | 0.29 |
| Total delivered RF energy (kcal) | 23.0 ± 4.0 | 16.9 ± 2.0 | 0.0005 |

**Note.**— Values are mean ± standard deviation. **P* stands for statistical difference between DSM-RFA and SSM-RFA groups. $D_m$ = minimum diameter of ablation zone, $D_M$ = maximum diameter of ablation zone, DSM-RFA = dual-switching monopolar radiofrequency ablation, $D_v$ = vertical diameter of ablation zone, SSM-RFA = single-switching monopolar radiofrequency ablation, $Volume_{eff}$ = effectively ablated volume

ablation volume (40.4 ± 16.4 $cm^3$) than that of SSM-RFA (20.8 ± 10.7 $cm^3$) for a given procedure time ($p < 0.0001$). Therefore, DSM-RFA with an SC electrode could be used for creating large coagulation areas with better efficiency delivering RF energy than those of the SSM-RFA technique. Furthermore, DSM-RFA created unified ablation zones in all cases, and most of the ablation zones were ideal oval/round shapes. No significant RFA-associated complications were observed. Therefore, we expect that DSM-RFA using a DS generator RF unit and an SC electrode may be an effective way to reduce local tumor progression in liver malignancies. Although further study is warranted to determine the

feasibility of DSM-RFA with an SC electrode, we expect that the DSM-RFA technique could be used in clinical practice for treating intermediate size (2–4 cm) malignant liver tumors with better tumor control rates.

The better performance of RFA using a DS system for creating a larger ablation zone with a better shape was mainly attributed to its greater efficiency for delivering RF energy at a given time. The mean values of the cumulative delivered RF energy were significantly higher in the DSM mode (23.0 ± 4.0 kcal) than those in the SSM mode (16.9 ± 2.0 kcal) ($p < 0.0001$). Several approaches have been proposed to increase the efficiency for delivering RF energy to target tissue, e.g., RFA using multiple electrodes, multi-tine electrodes, and saline perfusion electrodes (18, 19, 32). Although saline perfusion electrodes can improve the efficiency of RF energy delivery during the procedure by increasing the electric conductance, they could be limited by inhomogeneous distribution of saline within the target tissue which may result in an irregular shape of the ablation zones (33, 34). Therefore, RFA using multiple electrodes in simultaneous monopolar, switching monopolar, or bipolar and multipolar modes is regarded as a more controllable way to improve the efficiency of RF energy delivery than saline-perfused RFA, and it also creates large ablation zones (21, 28, 29, 35-38). In general, the greater efficiency of multiple electrode approaches costs more because of the use of multiple electrodes; it also limits the possibility of adjusting RF energy delivery to an individual electrode (26). DSM-RFA using an SC electrode and three-channel dual generator RF unit may provide several advantages compared with standard monopolar RFA using a single electrode or other multiple electrode approaches. The cost of an SC electrode is similar to that of a clustered electrode, and the cost of an SC electrode is less than the cost of three electrodes. In addition, the dual generator RF unit allows independent control of RF energy delivery to each individual electrode by monitoring impedance during the RFA procedure; it also permits the delivery of maximum RF energy to each of the electrode tips which is not possible with conventional RFA using a single generator system. Although previous studies have shown that conventional RFA using a single generator system and a standard cluster electrode or multi-tine electrode can improve the efficiency of creating a large ablation zone more than RFA using a single needle type electrode (9, 35), as they use synchronous energy application to a pair of electrodes, the maximum energy of any electrode is reduced equivalent to the number of electrodes used (Rule of Ohm) (26, 39).

Our results demonstrated that DSM-RFA at 2.0-cm or 2.5-cm IED could create united ablation zones in 12 minutes of RFA procedure time. As the simultaneous application of RF energy to the two electrode tips of an SC electrode could have the intrinsic problem of the Faraday's cage effect, which represents interference between multiple RF electrodes, identifying the ideal IED is crucial to create a unified, round/oval shaped ablation zone (26, 27). Considering that DSM-RFA at a 2.0 cm IED created a round or oval-shaped ablation zone in all lesions, we believe that a 2.0-cm IED could be the best for the 12-minute procedure time of DSM-RFA to overcome Faraday's cage effect. We also speculate that as the degree of tissue heating around each electrode in the DSM-RFA mode is strong enough to create sufficient thermal equilibrium rather than lethal cytotoxic temperatures (> 60°C) between the areas of active heating, this resulted in the creation of a confluent, single ablation area. However, there are some technical considerations to consider when performing DSM-RFA. First, although it is optimal to place the electrodes equidistant from each other to create a single, large ablation sphere, inserting three equidistant electrodes might be difficult for operators with less clinical experience (26). Electrical interference might be more severe with variable IEDs among the three electrode tips than seen in the cases with an equal distance between the electrodes. However, in our study, after an initial impedance rise of > 170% of baseline impedance, alternating DSM and SSM modes were used to prevent too rapid impedance rises during the RFA session, which was caused by high electrical current deposit around the electrodes, and to avoid impedance rises caused by possible electrical interference in the DSM mode. Second, using an SC electrode in a separated form is sometimes difficult depending on the tumor location and the patient's size. However, we surmised that inserting the electrodes before creating echogenic bubble clouds during RF energy instillation might be less challenging than performing overlapping ablations to replace the electrodes (16, 25).

Our experimental study had certain limitations. First, the small number of study animals was a major limitation. Second, the anatomy of the swine liver differs from that of human liver in that they are composed of four lobes that are separate and each lobe of the swine liver is smaller and thinner than those of a human liver. Therefore, the coagulation volume of DSM-RFA in our study might have been affected by liver thickness itself. Therefore,

Korean Journal of Radiology
KJR

extrapolating our results to human liver tumor could be limited. Despite these concerns, we believe that our results provide a reliable basis for future comparative studies regarding the efficiency of various RF modes in large animals *in vivo*, particularly the DSM mode, which provides a relatively larger amount of energy to tissue. Fourth, we tested the efficacy of SSM- or DSM-RFA using a 12-minute procedure time for creating large ablation zones, as if we increase the RFA time to longer than 24 minutes the DSM-RFA might be able to create a larger ablation zone than that seen in our study. Last, although we used intraoperative ultrasound for placing each electrode and for monitoring the ablation zone created, we did not obtain contrast-enhanced computed tomography (CT) or magnetic resonance images (MRI) to evaluate the possibility of thermal injury to the bile duct or intrahepatic vessels. Considering that creating large ablation zones with a single RF application is beneficial for achieving complete necrosis of an index tumor, it also has an increased risk of unexpected thermal injury to the adjacent vital structures. A thorough evaluation of thermal injury of the bile duct or hepatic vessels using three-dimensional, contrast-enhanced CT or MRI might have improved the quality of this study.

In conclusion, DSM-RFA using an SC electrode is feasible and enables the creation of larger ablation zones than SSM-RFA by allowing a larger RF energy delivery at a given time.

### Acknowledgments

We thank Bonnie Hami, M.A. (USA), for her editorial assistance, and Dong Eon Kim, B.A. (Korea) for his technical assistance in the animal experiments.

## REFERENCES

1. Lencioni R, Crocetti L, Pina MC, Cioni D. Percutaneous image-guided radiofrequency ablation of liver tumors. *Abdom Imaging* 2009;34:547-556
2. Lencioni R. Loco-regional treatment of hepatocellular carcinoma. *Hepatology* 2010;52:762-773
3. Cho YK, Kim JK, Kim MY, Rhim H, Han JK. Systematic review of randomized trials for hepatocellular carcinoma treated with percutaneous ablation therapies. *Hepatology* 2009;49:453-459
4. Forner A, Llovet JM, Bruix J. Hepatocellular carcinoma. *Lancet* 2012;379:1245-1255
5. Livraghi T, Meloni F, Di Stasi M, Rolle E, Solbiati L, Tinelli C, et al. Sustained complete response and complications rates after radiofrequency ablation of very early hepatocellular carcinoma in cirrhosis: is resection still the treatment of choice? *Hepatology* 2008;47:82-89
6. European Association For The Study Of The Liver; European Organisation For Research And Treatment Of Cancer. EASL-EORTC clinical practice guidelines: management of hepatocellular carcinoma. *J Hepatol* 2012;56:908-943
7. Peng ZW, Lin XJ, Zhang YJ, Liang HH, Guo RP, Shi M, et al. Radiofrequency ablation versus hepatic resection for the treatment of hepatocellular carcinomas 2 cm or smaller: a retrospective comparative study. *Radiology* 2012;262:1022-1033
8. Kuvshinoff BW, Ota DM. Radiofrequency ablation of liver tumors: influence of technique and tumor size. *Surgery* 2002;132:605-611; discussion 611-612
9. Livraghi T, Goldberg SN, Lazzaroni S, Meloni F, Ierace T, Solbiati L, et al. Hepatocellular carcinoma: radio-frequency ablation of medium and large lesions. *Radiology* 2000;214:761-768
10. Waki K, Aikata H, Katamura Y, Kawaoka T, Takaki S, Hiramatsu A, et al. Percutaneous radiofrequency ablation as first-line treatment for small hepatocellular carcinoma: results and prognostic factors on long-term follow up. *J Gastroenterol Hepatol* 2010;25:597-604
11. Solmi L, Nigro G, Roda E. Therapeutic effectiveness of echo-guided percutaneous radiofrequency ablation therapy with a LeVeen needle electrode in hepatocellular carcinoma. *World J Gastroenterol* 2006;12:1098-1104
12. Shiina S, Teratani T, Obi S, Sato S, Tateishi R, Fujishima T, et al. A randomized controlled trial of radiofrequency ablation with ethanol injection for small hepatocellular carcinoma. *Gastroenterology* 2005;129:122-130
13. Mazzaferro V, Battiston C, Perrone S, Pulvirenti A, Regalia E, Romito R, et al. Radiofrequency ablation of small hepatocellular carcinoma in cirrhotic patients awaiting liver transplantation: a prospective study. *Ann Surg* 2004;240:900-909
14. Lopez PM, Villanueva A, Llovet JM. Systematic review: evidence-based management of hepatocellular carcinoma--an updated analysis of randomized controlled trials. *Aliment Pharmacol Ther* 2006;23:1535-1547
15. Pompili M, Saviano A, de Matthaeis N, Cucchetti A, Ardito F, Federico B, et al. Long-term effectiveness of resection and radiofrequency ablation for single hepatocellular carcinoma ≤3 cm. Results of a multicenter Italian survey. *J Hepatol* 2013;59:89-97
16. Dodd GD 3rd, Frank MS, Aribandi M, Chopra S, Chintapalli KN. Radiofrequency thermal ablation: computer analysis of the size of the thermal injury created by overlapping ablations. *AJR Am J Roentgenol* 2001;177:777-782
17. Chen MH, Yang W, Yan K, Zou MW, Solbiati L, Liu JB, et al. Large liver tumors: protocol for radiofrequency ablation and its clinical application in 110 patients--mathematic model, overlapping mode, and electrode placement process. *Radiology* 2004;232:260-271
18. Mulier S, Miao Y, Mulier P, Dupas B, Pereira P, De Baere T, et al. Electrodes and multiple electrode systems for radio frequency ablation: a proposal for updated terminology. *Adv Exp Med Biol* 2006;574:57-73

19. Ni Y, Mulier S, Miao Y, Michel L, Marchal G. A review of the general aspects of radiofrequency ablation. *Abdom Imaging* 2005;30:381-400
20. Lee J, Lee JM, Yoon JH, Lee JY, Kim SH, Lee JE, et al. Percutaneous radiofrequency ablation with multiple electrodes for medium-sized hepatocellular carcinomas. *Korean J Radiol* 2012;13:34-43
21. Laeseke PF, Sampson LA, Haemmerich D, Brace CL, Fine JP, Frey TM, et al. Multiple-electrode radiofrequency ablation creates confluent areas of necrosis: in vivo porcine liver results. *Radiology* 2006;241:116-124
22. Frericks BB, Ritz JP, Roggan A, Wolf KJ, Albrecht T. Multipolar radiofrequency ablation of hepatic tumors: initial experience. *Radiology* 2005;237:1056-1062
23. Lee JM, Han JK, Kim HC, Choi YH, Kim SH, Choi JY, et al. Switching monopolar radiofrequency ablation technique using multiple, internally cooled electrodes and a multichannel generator: ex vivo and in vivo pilot study. *Invest Radiol* 2007;42:163-171
24. Woo S, Lee JM, Yoon JH, Joo I, Kim SH, Lee JY, et al. Small- and medium-sized hepatocellular carcinomas: monopolar radiofrequency ablation with a multiple-electrode switching system-mid-term results. *Radiology* 2013;268:589-600
25. Lee ES, Lee JM, Kim WS, Choi SH, Joo I, Kim M, et al. Multiple-electrode radiofrequency ablations using Octopus® electrodes in an in vivo porcine liver model. *Br J Radiol* 2012;85:e609-e615
26. Yoon JH, Lee JM, Han JK, Choi BI. Dual switching monopolar radiofrequency ablation using a separable clustered electrode: comparison with consecutive and switching monopolar modes in ex vivo bovine livers. *Korean J Radiol* 2013;14:403-411
27. Lee FT Jr, Haemmerich D, Wright AS, Mahvi DM, Sampson LA, Webster JG. Multiple probe radiofrequency ablation: pilot study in an animal model. *J Vasc Interv Radiol* 2003;14:1437-1442
28. Lee ES, Lee JM, Kim KW, Lee IJ, Han JK, Choi BI. Evaluation of the in vivo efficiency and safety of hepatic radiofrequency ablation using a 15-G Octopus® in pig liver. *Korean J Radiol* 2013;14:194-201
29. Lee JM, Han JK, Kim SH, Choi SH, An SK, Han CJ, et al. Bipolar radiofrequency ablation using wet-cooled electrodes: an in vitro experimental study in bovine liver. *AJR Am J Roentgenol* 2005;184:391-397
30. Laeseke PF, Sampson LA, Frey TM, Mukherjee R, Winter TC 3rd, Lee FT Jr, et al. Multiple-electrode radiofrequency ablation: comparison with a conventional cluster electrode in an in vivo porcine kidney model. *J Vasc Interv Radiol* 2007;18:1005-1010
31. Lee JD, Lee JM, Kim SW, Kim CS, Mun WS. MR imaging-histopathologic correlation of radiofrequency thermal ablation lesion in a rabbit liver model: observation during acute and chronic stages. *Korean J Radiol* 2001;2:151-158
32. Lee JM, Han JK, Lee JY, Kim SH, Choi JY, Lee MW, et al. Hepatic radiofrequency ablation using multiple probes: ex vivo and in vivo comparative studies of monopolar versus multipolar modes. *Korean J Radiol* 2006;7:106-117
33. Lee JM, Han JK, Chang JM, Chung SY, Kim SH, Lee JY, et al. Radiofrequency ablation of the porcine liver in vivo: increased coagulation with an internally cooled perfusion electrode. *Acad Radiol* 2006;13:343-352
34. Lee JM, Han JK, Kim SH, Shin KS, Lee JY, Park HS, et al. Comparison of wet radiofrequency ablation with dry radiofrequency ablation and radiofrequency ablation using hypertonic saline preinjection: ex vivo bovine liver. *Korean J Radiol* 2004;5:258-265
35. Appelbaum L, Sosna J, Pearson R, Perez S, Nissenbaum Y, Mertyna P, et al. Algorithm optimization for multitined radiofrequency ablation: comparative study in ex vivo and in vivo bovine liver. *Radiology* 2010;254:430-440
36. Laeseke PF, Sampson LA, Haemmerich D, Brace CL, Fine JP, Frey TM, et al. Multiple-electrode radiofrequency ablation: simultaneous production of separate zones of coagulation in an in vivo porcine liver model. *J Vasc Interv Radiol* 2005;16:1727-1735
37. Baldwin K, Katz SC, Rubin A, Somasundar P. Bipolar radiofrequency ablation of liver tumors: technical experience and interval follow-up in 22 patients with 33 ablations. *J Surg Oncol* 2012;106:905-910
38. Clasen S, Rempp H, Schmidt D, Schraml C, Hoffmann R, Claussen CD, et al. Multipolar radiofrequency ablation using internally cooled electrodes in ex vivo bovine liver: correlation between volume of coagulation and amount of applied energy. *Eur J Radiol* 2012;81:111-113
39. Lee JM, Han JK, Kim HC, Kim SH, Kim KW, Joo SM, et al. Multiple-electrode radiofrequency ablation of in vivo porcine liver: comparative studies of consecutive monopolar, switching monopolar versus multipolar modes. *Invest Radiol* 2007;42:676-683